Reference Data Generation of Spray Characteristics in Relation to Large 2-Stroke Marine Diesel Engines Using a Novel Spray Combustion Chamber Concept

K. Herrmann[*], B. von Rotz[*], R. Schulz[*], G. Weisser[*], K. Boulouchos[†] and B. Schneider[†]
[*] Wärtsilä Switzerland Ltd, PO Box 414
CH-8401 Winterthur, Switzerland
[†] ETH Zürich, Aerothermochemistry and Combustion Systems Laboratory
CH-8092 Zürich, Switzerland

Abstract

The availability of appropriate reference data for combustion in large 2-stroke marine diesel engines is a prerequisite for the further development of Computational Fluid Dynamics tools. In order to enable the acquisition of such data at relevant physical dimensions (bore) and operational parameters (pressure, temperature), including flow characteristics (swirl) and the low fuel qualities involved, a novel experimental test facility has been realized. The core element is a disk-shaped constant volume spray combustion chamber of diameter 500 mm with peripheral injection into a swirl flow. Thermo- and fluid dynamic conditions at start of injection similar to those in real engines are achieved by feeding the chamber via inclined intake channels with pressurized and heated process gas provided by a pressure vessel/heat regenerating system. The chamber design includes comprehensive possibilities for optical access as well as various injector arrangement options and the injection system is prepared for running on typical marine fuels. Reference data for the fuel spray propagation has been acquired by means of shadow-imaging measurements: This involved the variation of key parameters such as gas pressure and temperature (up to 9 MPa, 930 K), number of injector orifices and the spray orientation (10 deg counter- to 40 deg co-swirl) of a single-hole nozzle relative to the gas flow. The spray propagation data collected at conditions representative of the operation of large 2-stroke marine diesel engines contributes to a better understanding of the underlying phenomena and enables the validation of simulation tools at such conditions.

Introduction

Limitations continue to apply for the utilization of currently available Computational Fluid Dynamics (CFD) tools for the combustion system development and optimization of large 2-stroke marine diesel engines (e.g. [1]), despite the fact that promising results have been reported [2–4] in recent years. The mere dimensions (bore/stroke up to 960/3150 mm), time scales (down to 61 rpm) and specifics (e.g. injector size, nozzle hole sizes up to 1 mm and above) already constitute a major challenge for the application of the models developed for considerably smaller engines running at higher speeds and using fuel of much higher quality than customary fuels used in marine diesel engines.

Various investigations using optically accessible engines or motored devices [5, 6] are reported to study injection processes such as mixture formation, ignition and combustion. Additionally, in order to realize an improved optical accessibility and with regard to simpler boundary conditions, other test rig concepts have been defined. Some combustor vessels are designed as open flow-through constant pressure systems [7, 8], which yield a high repetition rate but cannot reproduce the pressure rise following the ignition, flame establishment and the heat release. Therefore, other optically accessible closed chamber concepts such as rapid compression machines [9, 10] or high-temperature pressure constant volume vessels [11–13] have been employed for a range of investigations [14, 15].

Note that the spray models used so far have commonly been validated against data from those small spray combustion chambers operating on high-grade fuels at conditions representative of smaller (automotive, truck, train) engines. Therefore, there have been various attempts to develop further experimental setups allowing the investigation of spray processes reflecting the situation in large marine diesel engines [16–20]; however, none of them has proven capable so far to fulfil the complete set of requirements for being considered adequately representative of the combustion system of large 2-stroke engines. Hence, relevant validation data for those applications, in view of their physical dimensions and operational parameters, were not available so far.

Therefore, in the context of the HERCULES research program [21] funded under EC's Framework Programmes [22], in order to study combustion processes at conditions typical of large 2-stroke marine diesel engines, a novel test facility [23] involving the following features has been realized:

- Combustion chamber of sufficiently large dimensions, pronounced swirl flow pattern of the gas phase

* Corresponding author: kai.herrmann@wartsila.com

- Peripheral injection via multiple orifices of different orientation and varying size of the individual orifices, with the option of simulating a two- or three-injector configuration
- Pressure and temperature levels at start of injection (SOI) exceeding 12 MPa and 900 K
- Fuel system able to cope with a wide range of (low) fuel qualities

In order to satisfy the usual requirements with respect to the application of both standard and (laser-) optical technologies for the generation of validation data, the combustion chamber needed to be equipped with appropriately sized and located windows for allowing optical access to all regions of interest and the vicinity of the injector in particular.

Test Facility Setup

An optically accessible constant volume chamber of diameter 500 mm has been designed [23], which is representative of the dimensions of smaller 2-stroke as well as larger 4-stroke marine diesel engines. This test facility allows an optical investigation of in-cylinder processes such as fuel injection and evaporation, ignition, combustion and emission formation. In order to achieve realistic conditions at the start of injection, the pressurized air (or N_2 for inert investigations) fed into the chamber through inclined inlet ports is preheated in an adjacent pressure vessel/heat regenerating system.

Figure 1 (left) shows the schematic drawing of the test facility setup. A pressure vessel system equipped with fast opening valves feeds process gas via a so-called regenerator to the spray combustion chamber. The inner core of this regenerator consists of a tensioned package of electrically heated discs with clusters of plates in between and is insulated against the housing by ceramic rings. Two types of those heat disks are used in order to enforce a labyrinth type flow of the process gas inside the regenerator. The radial passages for the flow between two neighbouring heat discs as well as the heat flux from the disks to the plates are provided by triangular distance plates fitted between the individual plates and disks. This assembly results in a high overall surface to volume ratio in order to achieve an optimum heat transfer from the heated core. The flow through the tilted intake channel generates engine similar swirl in the spray combustion chamber, through appropriate selection of angle and flow area. The fast filling process in combination with the heated chamber walls ensures lower heat losses. Shortly before the desired initial pressure in the chamber is reached, the accumulator valves close and injection starts, followed by combustion in the reactive cases. Finally, the exhaust valve opens, the regenerator is heated up again, and a compressor is refilling the accumulator with air or nitrogen within a few minutes, which are also required for reheating the regenerator.

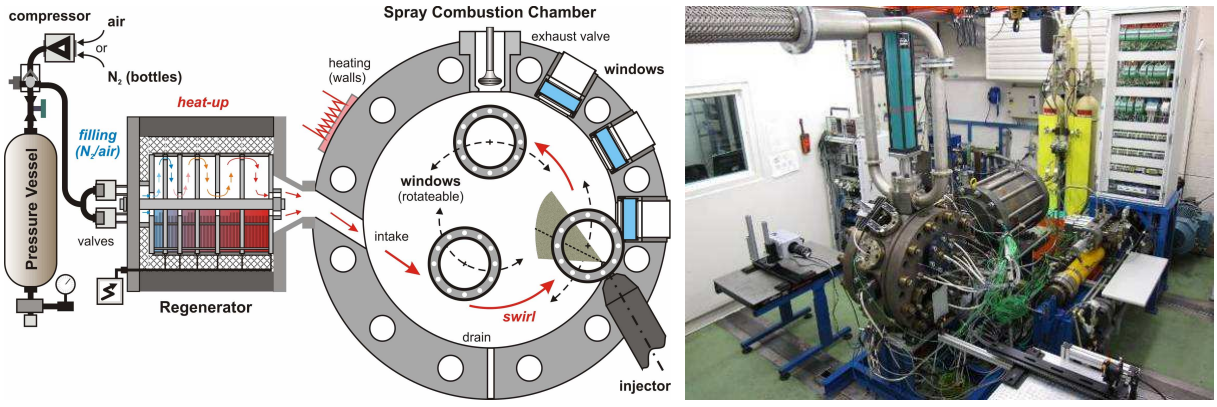

Figure 1 Schematic drawing and principle of the experimental setup (left), indicating operational (filling, heat up, swirl, injection) and functional aspects (window position, exhaust valve) and the genuine spray combustion chamber test facility (right).

Note that the intake channel remains open throughout the process to allow a certain expansion of the combustion chamber content and thus attenuating the limitations with respect to the maximum pressure otherwise applicable to the isochoric combustion chamber. The regenerator thereby acts as a flame arrester while the burnt gases flowing back assist in its reheating. The exhaust valve (actuated by a pneumatic cylinder) opens to the exhaust side and enables blowing off in case the pressure in the chamber exceeds a critical value. A drain valve is fitted at the bottom of the chamber for evacuating unburnt fuel in case of inert (N_2) investigations. Fuel admission is realized through one or two injectors located at mid-height of the chamber on its circumference, which are fed by an injection system (common rail, pressure up to 100 MPa) similar to those installed on the most recent production engines.

Figure 1 (right) gives an impression of the entire test facility setup including various subsystems. The spray combustion chamber (Ø500x150 mm) consists of a main body and two cover plates, which both include three

holes each, where windows or cover dummies (containing heating cartridges or pressure and temperature sensors) can be mounted. It is designed to handle pressures up to 20 MPa peak firing pressure and is equipped with heating cartridges to maintain a wall temperature of approximately 200 °C. The three holes of the covers are located at different radial positions relative to the axis of rotation, starting from an outer position where the tip of the injector is within the observation area. Optical access (∅100 mm) is granted by sapphire windows, which can be rotated in sufficiently small incremental steps of 15 degrees relative to the body of the chamber. The design of the main body also includes three holes for mounting standard injectors as applied on engines of that size: In addition to one baseline location foreseen at the bottom right of the chamber, two additional locations (not included in the schematic representation of the combustion chamber in Figure 1) above and below the intake channels are provided. This allows reproducing the 120 and 180 degree angular distance of the atomizers as present in the three- or two-injector configurations commonly used on engines, which thus enables the investigation of interaction effects of sprays originating from different injectors.

The pressure accumulator bottles, connected to the regenerator behind the spray combustion chamber, can be recognized at the rear of Figure 1 (right). The common rail injection system is currently operated on light fuel oil (see Table 1) but is prepared for the use of different fuels (including HFO). Its main components are located up rear where on the right side the electrical motor of the high-pressure pump feeding the fuel rail can be seen. The latter is located beside the regenerator, lying underneath an electrical cabinet used for control device signal collection and distribution. The control room is located behind the wall to the left, where a bullet-proof window allows the observation of the spray combustion chamber during operation. The control cabinet inside (partly visible) is connected to another electrical cabinet (located next to the window) used for measurement data signal collection.

Operation and Validation

When operating the test facility, pressure, temperature and swirl in the spray combustion chamber at SOI can be adjusted by varying the accumulator pressure and/or the opening valve timing and the regenerator core temperature. In order to verify the proper operation of the entire setup, the conditions of the process gas, the fuel injection system, heated or pressurized components as well as positions of switches, valves or other devices are monitored extensively. Pressure data acquisition is performed by means of water-cooled piezoelectric sensors at different positions, calibrated at each filling process by a piezoresistive one. Temperatures are measured with standard Type K sheath thermocouples, using such with 0.5 mm diameter at critical locations for an optimum of response time and durability.

The setup has been validated thoroughly against the requirement specifications and its applicability for the intended purpose could be completely confirmed [24]. For this purpose, flow measurements by means of laser Doppler velocimetry (LDV) have been combined with the standard monitoring techniques mentioned above. An LDV system specified for velocity measurements up to 150 m/s has been applied at a radial position of the measurement point on the centre plane at 200 mm from the chamber axis. The swirl level target velocity range is reached between 0.6 s and 1.0 s after starting the blow-down of the process gas via the regenerator by actuating the fast-opening valves at the pressure accumulator bottles. With an accumulator pressure of >300 bar, a valve actuating time between 400 ms and 750 ms, a regenerator inner core temperature of 920° C, pressure and temperature levels of up to 13 MPa and more than 930 K (before injection/combustion) as well as the swirl level target velocity range (15-25 m/s) can be achieved at the same time, thus allowing the simultaneous realization of typical values of the key engine combustion parameters.

Methodology and initial application

The spray propagation inside the chamber has been visualized by means of an improved "Shadow-imaging" method using a pulsed diode laser (690 nm) light source. Due to the very short 50 ns laser pulse within a 1 μs exposure time of a high-speed CMOS-camera (20 kHz frame rate, 512x512 pixel) in combination with an appropriate narrow band pass filter (CWL 689.1 nm, T 60%, FWHM 10.6 nm), a high signal-to-noise ratio in the recordings is achieved. Due to the short exposure time, the flame light is almost completely suppressed and spray visualization becomes feasible even under reactive conditions. As a consequence, considerably "sharper" images are obtained and it is possible to continue observation of sprays even after ignition has taken place.

In a first stage, the illumination and observation windows were mounted in the outer position for obtaining optical access to the region directly adjacent to the injector tip in order to allow the observation of the initial spray propagation. Figure 2 shows a selection of (reactive case) spray evolution imaging series with time step of 50 μs for various spray configurations at otherwise unchanged conditions (9 MPa, 930K): The upper four series refer to single-hole nozzle cases with spray orientation varying from 10 deg counter-swirl (first row) and an orientation perpendicular to the swirl (second row) via a 15 deg co-swirl case to an injector-co-axial orientation (fourth row). The next three series originate from two-hole nozzle cases with identical orifice diameters and angles between the individual sprays but again varying the overall orientation from more counter-swirl to co-swirl

variants. The last series then refers to a five spray case representative of injectors typically used on engines of similar size with pronounced orifice size distribution (decreasing with co-swirl orientation). The irregular and random nature of the spray is clearly visible in the formation of well-defined structures at its boundaries, which requires proper consideration in the (statistical) analysis of the shadow imaging data.

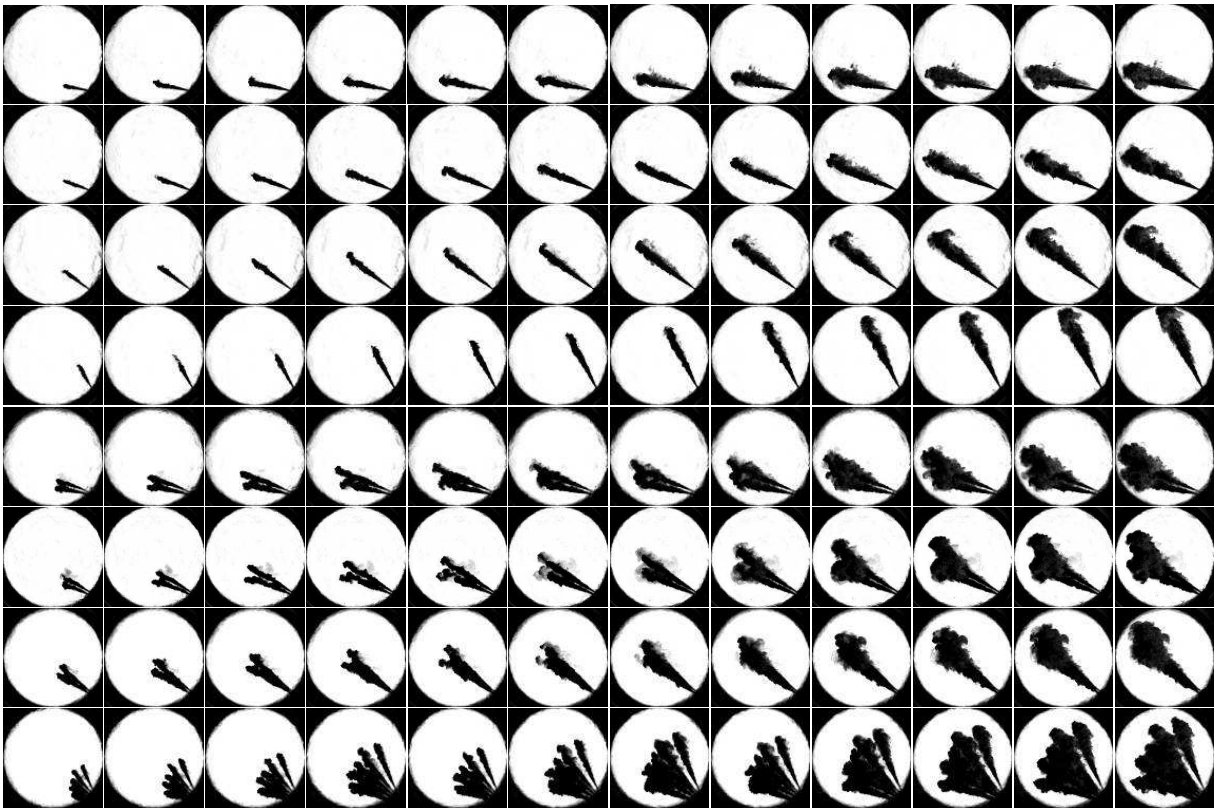

Figure 2 Shadow-images of the temporal spray plume evolution for a variety of spray configurations at identical combustion chamber conditions (9 MPa, 930K).

Before even going into the in-depth analysis of the data as outlined below, clear differences can already be identified by mere visual comparison: The effect of spray orientation is materializing in reduced penetration with counter-swirl orientation, whereas the width of the plume is clearly increased compared to the co-swirl cases. When looking at the two-hole nozzle configurations, one observes a striking difference in the propagation of the two sprays: The more counter-swirl oriented spray in all cases exhibits a clearly shorter penetration than the more co-swirl oriented one. Such difference is in principle in line with the observations made above; however, the difference is much more pronounced than the single-hole nozzle data would suggest. Hence, there seems to be a kind of shielding effect exerted by the more counter-swirl oriented spray, which reduces the interaction of the second spray with the baseline flow in the combustion chamber, resulting in a longer conservation of the initial momentum of this spray. This effect is also present in the five spray case, where the penetration of the sprays increases with more pronounced co-swirl orientation – in spite of the fact that the decreasing orifice sizes generally result in lower penetration.

Measurement campaigns and analysis

An extensive number of systematic measurements for determining the spray evolution and ignition behaviour at various chamber conditions (pressure, temperature) and injection parameters (nozzle tip configuration), including inert investigations by using nitrogen as process gas, have been performed. In particular, the single-hole nozzle cases at various orientations of the spray relative to the swirl have been analysed in detail in order to obtain initial quantitative reference data with respect to the spray evolution (penetration, angle). Table 1 gives an overview of the experimental settings with regard to injector (nozzle) and operational parameters (p, T) and the properties of the used light fuel oil. The single-hole nozzle bore diameter is 0.875 mm in all cases, whereas the nozzle hole exit (defined to be zero perpendicular to the injector axis) is varying from co-axial (90°) to co-swirl (65°), via swirl-perpendicular (50°) to a counter-swirl configuration (40°). The pressure and temperature conditions were kept at 9 MPa / 930 K. For the 50 deg and 90 deg cases pressures of 6 and 3 MPa have also been taken into account. Note that, with identical operation settings (e. g. regenerator temperature), the resulting tem-

peratures are slightly reduced to 920, resp. 900 K. The injection pressure has been set to 1000 bar in order to assure comparable injection behaviour as in marine diesel engine multiple-hole nozzle injection systems.

Hole ⌀ d_0 [mm]	Angle [deg]	Comments	Pressure p [MPa]
0.875	90	Injector co-axial	9/6/3
0.875	65	15° co-swirl	9
0.875	50	Swirl-perpendicular	9/6/3
0.875	40	10° counter-swirl	9
Process gas: nitrogen (N_2) Accumulator pressure: 300/180/100 [bar] Regenerator temperature: 920 [°C] Intake valve actuating time: 400 [ms] Swirl flow level: 15 – 25 [m/s] Combustion chamber temperature: 900 – 930 [K] Injection pressure: 1000 [bar]			

Properties	Unit	Value	Method
Density at 15°C	kg/m^3	851.4	ISO 12185
Viscosity at 40°C	mm^2/s	2.928	ISO 3104
Viscosity at 80°C	mm^2/s	1.522	ISO 3104
Gross Heat of Combustion	MJ/kg	45.02	ASTM D240
Water Content	% V/V	<0.10	ASTM D6304
Carbon Residue (10% Bottom)	% m/m	<0.10	ISO 10370
Sulfur	% m/m	0.09	ISO 8754
Ash	% m/m	<0.01	LP 1001
Flash Point	°C	58	ISO 2719
Pour Point	°C	<-6	ISO 3016
Calculated Cetane Index	-	47	ISO 4264

Table 1 Injector nozzle specifications and operation parameter (left) and fuel specifications (right) of the used light fuel oil.

Due to the large size of the spray combustion chamber and the practical limitations regarding window size, data from several measurement series have to be superimposed, where the window position was adjusted between series at otherwise unchanged conditions in order to enable the observation of the entire spray evolution, especially at lower pressure conditions. This procedure is illustrated in Figure 3, showing a sketch of the combustion chamber, including indications of the axes of the individual sprays and the window positions used. In addition, four typical examples of assembled cases with respect to different chamber pressure and nozzle tip are shown. The good qualitative agreement of the individual measurements is highlighted when considering the regions where the images from the different measurement series overlap, thus confirming also the high level reproducibility.

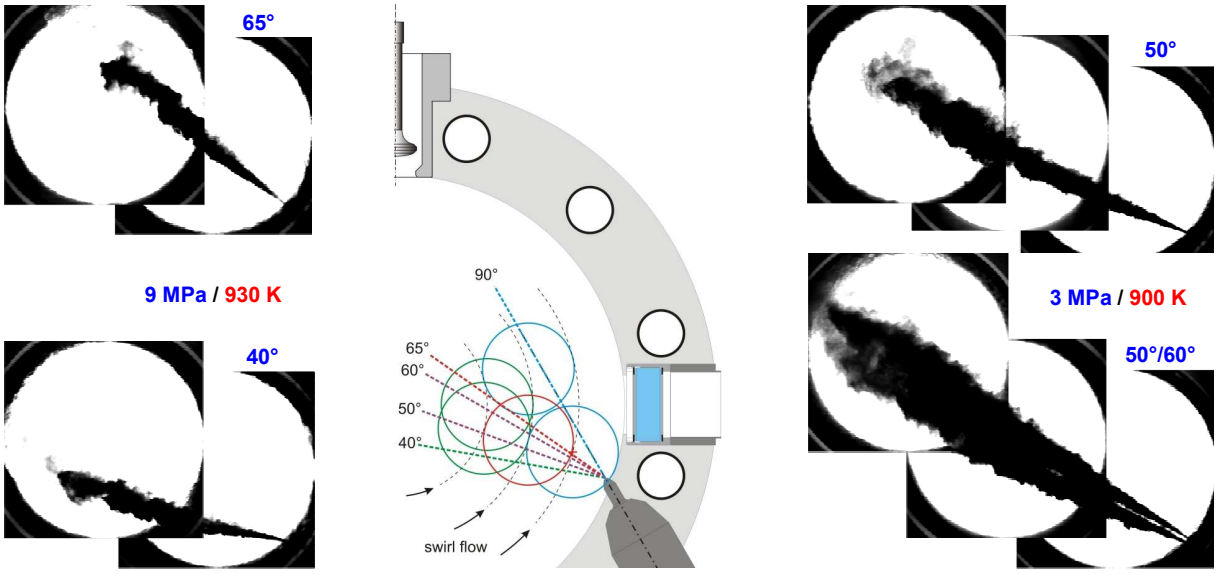

Figure 3 Sketch of the spray combustion chamber indicating the different overlapping measurement locations (window) positions, together with some examples of assembled spray plume evolutions.

The accurate detection of the spray tip penetration and the cone angles is performed by image processing of the recorded data sets. The sub-steps involved include background subtraction, image intensity distribution correction and subsequently peak-stretching to ensure the comparability between all images recorded in separate injection sequences. As the position of the spray contour is directly dependent on the minimum detectable droplet concentration, a certain percentage of the background gray scale value is employed for its definition, in accordance with common practice [14]. Figure 4 (left) exemplifies this procedure for the case of a single, injector co-axial spray: The original image is rotated by 120° in order to horizontally align the axis of the spray. Then, thresholds of 90% (spray contour) and 10% (dense core) of the background gray scale level are applied for determining the spray outlines. The penetration is obtained by measuring the (horizontal) distance from the nozzle

tip to the leading edge of the spray – it is worthwhile noting that in this case, the contours of the spray and its dense core virtually coincide at the spray tip. The identification of cone angle is clearly more difficult – in fact, four or even five such angles can be defined: Due to the strong swirl, the spray is deflected, resulting in different angles relative to the original axis on the windward ("luv") side of the spray and the side sheltered from the swirl ("lee"). Whereas this effect is virtually negligible for the dense core, it is quite pronounced for the complete spray and we consequently define "lower" (luv side) as well as "upper" (lee side) and total values for the cone angle, which are analysed at various distances x/d_0 from the injector tip. In order to account for these special characteristics of the setup, the capabilities of the analysis software [14] employed have been extended accordingly. On the right side of Figure 4 another important step of the post-processing is displayed: In order to quantify the magnification (pixel vs. mm), to be able to assemble all the overlapping measurements and to define the origin of the large spray for the calculation of the penetration as well as the angles, several scale images need to be defined and positioned at the correct location.

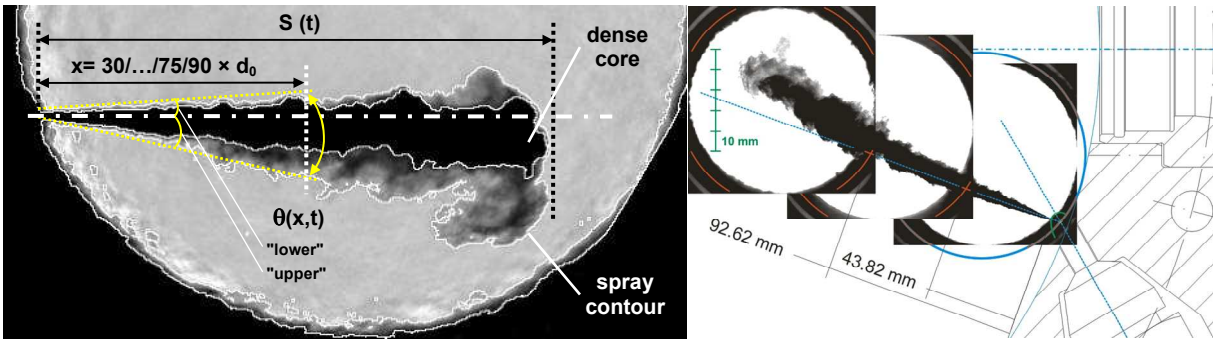

Figure 4 Analysis of spray penetration and cone angles (total, "upper", "lower") on the basis of two threshold levels (spray contour, dense core) and post-processing procedure (scale image).

Despite the fact that the entire setup is operating in a highly repeatable manner, shot-to-shot variations cannot be entirely excluded and are arising particularly from fluctuations in the injection system. This can result in slight deviations of the actual start of injection, even for identical timing of the injection actuation due to hydraulic delays caused by the working principle (spring against opening pressure) of the injector. Each injection is a separate process which is adjusted to the others on the basis of the simultaneously acquired needle lift signal. As a consequence, the time base is corresponding to the start of the needle lift (SONL). The final analysis of spray penetration and cone angle evolution for a complete measurement series is then based on the statistical evaluation (median) of the data obtained in the individual sequences of the series.

Results and Discussion

In Figure 5, the spray penetration (contour/dense core, left) and the cone angle (contour, right) of the single-hole injector co-axial nozzle under variation of the chamber pressure (9/6/3 MPa, 930/920/900 K) is shown.

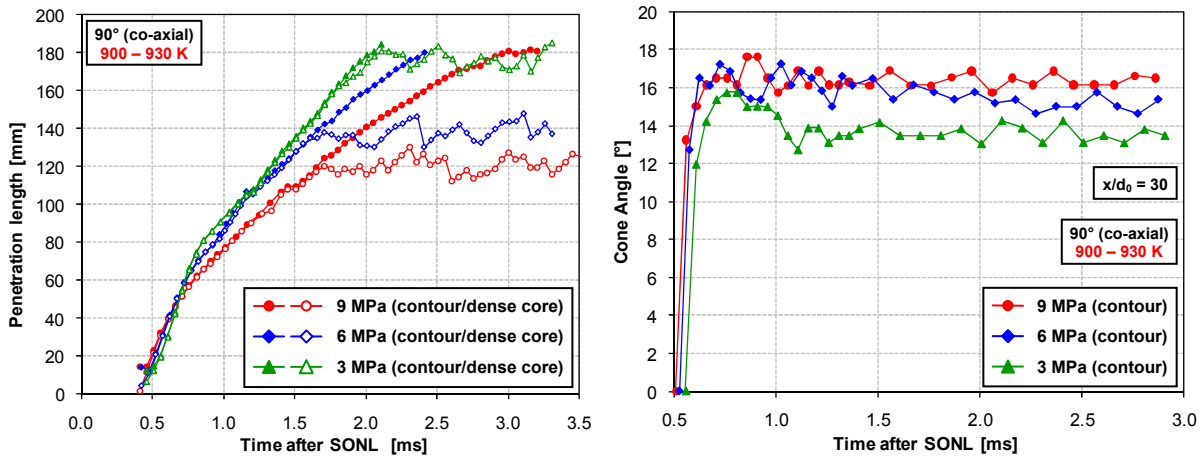

Figure 5 Spray penetration (contour/dense core, left) and total cone angle (contour, right) of the single-hole injector co-axial nozzle at x/d_0=30 under variation of the chamber pressure.

As is well-known from earlier investigations [25, 26] at smaller dimensions, the spray is propagating linearly along its axis during the initial phase, whereas, in the later propagation stage, its penetration is scaling with the

square root of time – hence, the gradient of the curve is decreasing. The spray contour and the dense core are separating at a certain level: Whereas the latter is stabilizing at this (case dependent) level, the spray contour tip continues to propagate and additional effects are becoming relevant (e.g. due to the action of the swirl), such that, for the high pressure case, the gradient is even further decreased during the later injection phase (> 2.5 ms). Reducing the chamber pressure from the above 9 MPa level results in higher injection velocity and therefore faster penetration during the initial phase. The total spray angle (Figure 5, right), by nature associated with more fluctuations, also exhibits some sensitivity to the above mentioned shot-to-shot variations; however, this is mostly the case for the first non-zero values established right after the spray arrives at the measurement location. Afterwards, an almost constant level is achieved which is dependent on the gas density in the chamber – an increasing chamber pressure is clearly associated with higher total cone angle values. Note that the total cone angle decreases as a function of x/d_0, as can be seen comparing the 9 MPa / 930 K case, displayed for $x/d_0 = 30$ in Figure 5 (right) and for $x/d_0 = 75$ in Figure 7 (right) below. Generally, a tendency that faster penetration is associated with smaller cone angles is recognizable.

The separation of the dense core and the spray contour penetration characteristics mentioned above is exemplarily illustrated in Figure 6. With increasing penetration of the spray, the plume is more and more affected by the acting aerodynamic forces – up to the point, when these are sufficiently high close to the tip of the spray to completely break up the liquid elements of the dense core. After this point, the spray continues to penetrate in the form of the droplet clouds created from the break-up of the dense core.

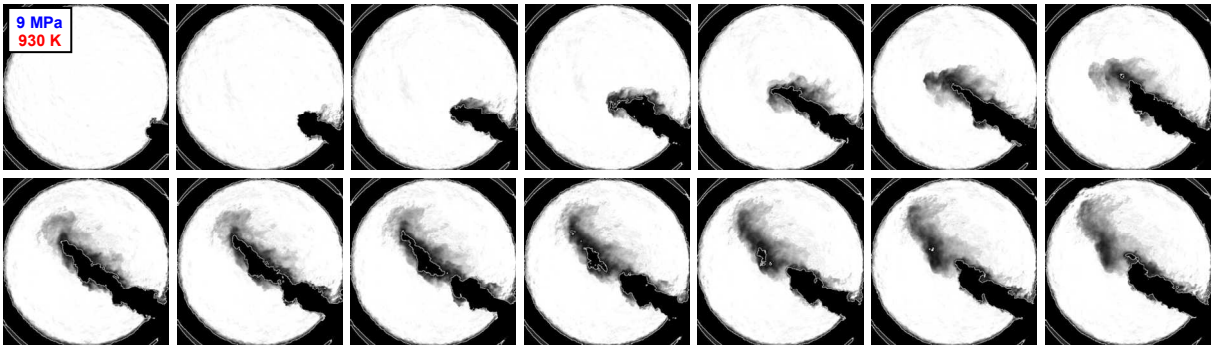

Figure 6 Visualization of the dense core break-up and its fluctuating maximum propagation.

Figure 7 shows a similar analysis for the effect of the orientation of a single-hole nozzle: When moving from a counter-swirl orientation (40°) via swirl-perpendicular (50°) towards co-swirl (65°, 90°) cases, the penetration tends to increase, whereas the development of the contour cone angle decreases. Here, also the good agreement of the results of the overlapping measurement locations is recognizable. Furthermore, the cone angle of the spray contour as well as of the dense core is displayed in Figure 7 (right). The swirl influence effects with respect to the spray orientation can be seen in the higher level of the established total cone angle of the 10 deg counter-swirl (40°) compared to the injector co-axial (90°) case at a position of x/d_0=75. In addition, also the increasing difference between the spray contour and dense core cone angle levels can be clearly recognized.

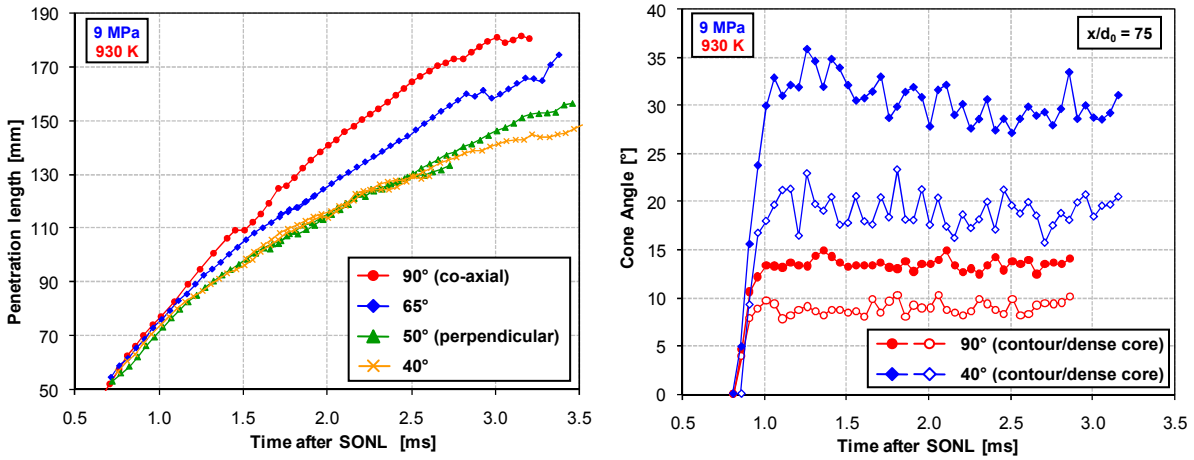

Figure 7 Penetration length with respect to different single-hole nozzle exit angles (left) and total cone angle (right): Comparison of the injector co-axial case (90 deg) and the 10 deg counter-swirl (40 deg) case at x/d_0=75 under 9 MPa / 930 K operation conditions.

Figure 8 gives a visual impression of the aerodynamic swirl force influence with regard to the dense core and the spray contour. The transition region is increased, especially at the lee side compared to luv side of the spray, and the cone angle is decreased as shown above.

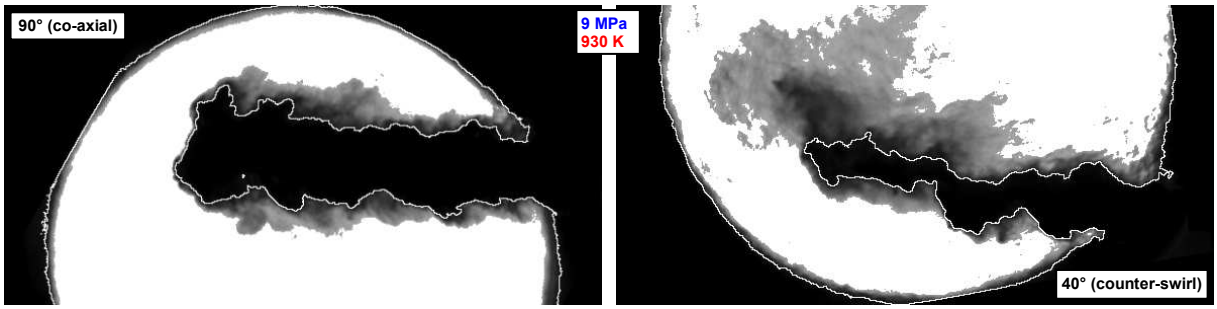

Figure 8 Spray contour and dense core of the injector co-axial case (90 deg) compared to the 10 deg counter-swirl (40 deg) case at 9 MPa / 930 K operation conditions.

Figure 9 shows the behaviour of the two "lower" and "upper" cone angles of the spray contour with respect of the swirl perpendicular (50°) case under the variation of pressure (left) and compared to the injector co-axial case (90°, right). The "upper" (lee side) cone angle is very much affected due to the swirl, whereas the "lower" (luv side) cone angle earlier remains at a basically constant lower level. The deflection of the spray plume under chamber pressure variations (9/6/3 MPa) is recognizable in the upper cone angle as well as in a less pronounced manner in the lower cone angle. The spray orientation influence is displayed in Figure 9 (right), where the counter-swirl case leads obviously to a much larger "upper" (lee side) cone angle of the spray contour than in the co-swirl case, whereas both "lower" cone angles again remain basically constant at a similar lower level. For the 50° case, again the effect of increasing cone angle with decreasing x/d_0 is recognizable.

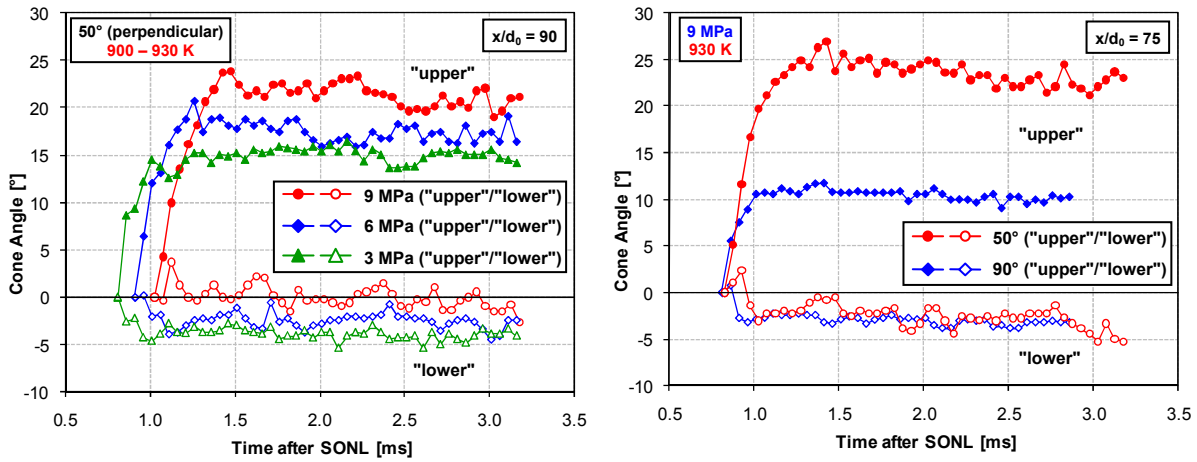

Figure 9 Comparison of "upper" and "lower" cone angles of the swirl-perpendicular case (50 deg) at x/d_0=90 for different chamber pressures (left) and compared to the injector co-axial (90 deg) case at x/d_0=75 under 9 MPa / 930 K operation conditions.

These comparisons represent only the most simple and straightforward examples of the data available now, but the results have already been used for the validation of CFD models and approaches [27]. The next steps will also involve an assessment against empirical spray propagation models. The investigations will be continued by studying similar variations for the two-hole nozzle configurations – including the effect of using non-identical orifice sizes. Last but not least, configurations closer to actual engine designs (e.g. five-hole nozzle) will be investigated.

Conclusions

A novel experimental setup, allowing the investigation of spray and combustion processes at conditions typical of large 2-stroke marine diesel engines, has proved its suitability for the generation of reference data for the validation of CFD models and approaches targeting such applications. The flexible adjustment possibilities satisfy the requirements towards versatility of the setup in terms of injector configuration and the location of the windows relative to the position of the injector allowing the observation of the entire spray evolution.

In a first step, shadow-imaging techniques have been applied for obtaining first sets of spray propagation data, which have been analyzed in order to determine relevant characteristics such as penetration and spray angles for a whole range of conditions. On the one hand, variations of chamber pressure in the range 3 up to 9 MPa at 900 to 930 K have been investigated. On the other hand, the orientation of the spray from a single-hole nozzle relative to the swirl has been varied between 10 deg counter-swirl and 40 deg co-swirl. In this context, the swirl influence on the different angles resulting from the spray deflection has been given particular attention.

The results of these analyses yield valuable insight into the behaviour of individual sprays at those conditions; however, further investigations are expected to contribute to an even better understanding of the complex phenomena involved, particularly with respect to spray interactions. Ultimately, the findings from such more in-depth analyses will help in developing models for allowing better predictions of combustion related phenomena in large 2-stroke marine diesel engines.

Acknowledgment

The present work has been conducted as part of the HERCULES-β project within EC's 7th Framework Program, Contract SCP7-GA-2008-217878. Financial support by the Swiss Federal Government (State Secretariat for Education and Research SER & Swiss Federal Office of Energy SFOE Contract 154269, Project 103241) is gratefully acknowledged.

References

[1] Weisser G., Schulz R., Wright Y., Boulouchos K., *CIMAC Congress*, Kyoto, Japan, June 2004, Paper No. 211.
[2] Rodatz P., Weisser G., Tanner F.X., *SAE Congress*, Detroit, USA, 2000, SAE 2000-01-0948.
[3] Endo H., Oda Y., Okabe M., Sakaguchi K., *CIMAC Congress*, Hamburg, Germany, May 2001, pp. 665-672.
[4] Kim C.S., Lee D.H., Cho Y.S., *CIMAC Congress*, Hamburg, Germany, May 2001, pp. 1141-1148.
[5] Bruneaux, G., Verhoeven, D., Baritaud, T., SAE 1999-01-3648 (1999)
[6] Desantes, J.M., Pastor, J.V., Payri, R., Pastor, J.M., *At. Sprays* 15:517–543 (2005)
[7] Koss, H.J., Brüggemann, D., Wiartalla, A., Bäcker, H., Breuer, A., *Final Report of JOULE Project on Integrated Diesel European Action* (IDEA), 1992.
[8] Vogel, S., Hasse, C., Gronki, J., Andersson, S., Peters, N., Wolfrum, J., Schulz, C., *Proc. Combust. Inst.* 30:2029–2036 (2005).
[9] Akiyama, H., Nishimura, H., Yasumitsu, I., Iida, N., *JSAE Rev.* 19:319–327 (1999).
[10] Balles, A., Heywood, J.B., SAE 880206 (1988).
[11] Pickett L.M., Siebers D.L., *Combustion and Flame* 138:114-135 (2004).
[12] Bruneaux G., *Atomization and Sprays* 11:533-556 (2001).
[13] Yu J., Bae C., Proc. Instn Mech. Engrs 217:1135-1144 (2003).
[14] Schneider B., *PhD thesis*, No. 15004, ETH Zurich, 2003.
[15] Wright Y.M., Margari O.-N., Boulouchos K., De Paola G., Mastorakos E., *Flow Turbulence Combust* 84:49-78 (2010).
[16] Negus C.R., Dale B.W., Stenhouse I.A., McNiven A.J., *CIMAC Congress*, Warsaw, Poland, 1987, Paper No. D-78.
[17] Takasaki K., Tajima H., Nakashima M., Ishida H., *CIMAC Congress*, Hamburg, Germany, May 2001.
[18] Nakagawa H., Oda Y., Kato S., Nakashima M., Tateishi M., *COMODIA 90*, pp. 281-286, 1990.
[19] Buchholz B., Pittermann R., Niendorf M., *CIMAC Congress*, Vienna, Austria, May 2007, Paper No. 129
[20] Imahashi T., Tomita E., Kimoto T., , *CIMAC Congress*, Vienna, Austria, May 2007, Paper No. 177
[21] Kyrtatos N.P., Kleimola M., Marquard R., *CIMAC Congress*, Vienna, Austria, May 2007, Paper No. 31.
[22] http://cordis.europa.eu
[23] Herrmann K., Schulz R., and Weisser G., *CIMAC Congress*, Vienna, Austria, May 2007, Paper No. 98.
[24] Herrmann K., Kyrtatos A., Schulz R., and Weisser G., *ICLASS 2009, 11th Triennial International Annual Conference on Liquid Atomization and Spray Systems*, Paper No. 005, Vail, Colorado USA, July 2009.
[25] Hiroyasu H., Arai M., SAE 900475 (1990).
[26] Naber J.D., Siebers D.L., SAE 960034 (1996).
[27] Schulz R., Herrmann K., von Rotz B., Hensel S., Seling F., Weisser G., Wright Y.M., Bolla M., Boulouchos K., *CIMAC Congress*, Bergen, Norway, June 2010, Paper No. 247.